

Additive manufacturing of titanium porous transport layers for enhanced performance in proton exchange membrane water electrolysis

Gerrit Ter Haar^{1*}, Craig McGregor¹

¹Mechanical and Mechatronic Engineering Department, Faculty of Engineering, Stellenbosch University, Stellenbosch, South Africa

Abstract. This study investigates the feasibility of using Laser Powder Bed Fusion (L-PBF) additive manufacturing (AM) to fabricate porous titanium Porous Transport Layers (PTLs) for Proton Exchange Membrane Water Electrolysis (PEMWE) systems. We explore L-PBF as a potential solution to overcome limitations of traditional PTL manufacturing methods, such as limited control over structural morphology and inefficient material use. Using spheroidized titanium powder, we produced 1 mm thick plates with varying porosities by manipulating laser process parameters. The internal structure and surface morphology of AM-produced PTLs were characterized and compared to conventional press-sintered PTLs. L-PBF successfully produced PTLs with porosities in the recommended 30-50% range, featuring spherical particles and a textured pore structure. *In-situ* testing in a lab-scale PEMWE revealed that AM-produced PTLs exhibited improved performance compared to commercial press-sintered PTLs. This enhancement is attributed to the finer surface structure and favourable gas-liquid transport properties of the AM-produced PTLs. These preliminary findings suggest that L-PBF is a promising method for manufacturing PTLs, offering potential advantages in design flexibility, material efficiency, and PEMWE performance. Further research is needed to fully optimize the AM process and comprehensively evaluate long-term PTL performance.

1 Introduction

The transition towards a sustainable energy future is critical in addressing the challenges of climate change and environmental degradation. The production of green hydrogen, which involves splitting water molecules using electricity from renewable sources, is gaining traction as a viable method for reducing carbon emissions across transportation, industrial processes, and energy storage applications. At the core lies the electrolyser technology, which harnesses electricity from renewable sources to split water molecules and generate hydrogen. However, the widespread adoption of green hydrogen faces several challenges, including the high materials and manufacturing costs of electrolysers [1]. In recent years, proton exchange membrane water electrolysers (PEMWE) have gained significant attention due to their high

* Corresponding author: gterhaar@sun.ac.za

efficiency, compact design, and ability to operate at high current densities and under dynamic load conditions [2]. These advantages have fuelled the surge in interest and investment in PEMWE, as they offer a promising solution for scalable green hydrogen production.

A crucial component of PEM electrolyzers is the liquid-gas diffusion layer (LGDL), also commonly called the porous transport layer (PTL), which serves multiple functions within the cell. These include two-phase transport of gas and water, thermal and electrical conductivity and mechanical support for the catalyst-coated membrane (CCM). Titanium and stainless steel are the preferred material due to their corrosive resistance and good electric properties. While PTL material composition primarily affects cell ohmic resistance, structural characteristics largely determine mass transport resistance [1]. These properties control the ease of gas and water movement through the PTLs. Recent research has focused on several key structural aspects, including porosity, pore diameter and structure, morphology, thickness, and permeability [1]. Findings from these studies have established that PTL structural properties are crucial determinants of PEMWE performance.

Sintered titanium is the most widely used material for Porous Transport Layers (PTLs) in Proton Exchange Membrane Water Electrolysis (PEMWE) systems. Researchers have undertaken numerous initiatives to optimize PTL structure for enhanced PEMWE performance. One key area of focus has been porosity, with studies indicating that optimal PTL porosity falls within the range of 30% to 50% [1,3]. In their study, Grigoriev et al. [4] investigated how various sintering properties affect PEMWE performance. Their findings revealed that titanium powder with particle sizes between 50 μm and 75 μm produces optimal results. After sintering, this particle size range yields PTLs with a porosity of 35% to 40%, which was found to be ideal for PEMWE operation.

The interface between the PTL and catalyst layer significantly influences cell performance in PEM water electrolyzers. To enhance catalyst layer utilization, recent research has focused on developing micro-porous layers (MPLs) using techniques such as sintering [5] or low-temperature air spraying [6]. Schuler et al. [5] created a hierarchically structured PTL by combining two layers: an MPL sintered from fine titanium powder (2–20 μm particle size) and a support layer made from coarser titanium powder (30–50 μm particle size).

Although progress has been made in understanding the structure-performance correlations and the application of this knowledge to novel designs, for example the MPLs, the traditional manufacturing methods still have limited control over structural morphology, pore size distribution and PTL-cell integration. Furthermore, traditional methods are costly, inefficient and energy intensive. The current study investigates the additive manufacturing (AM) process of laser powder bed fusion (L-PBF) as a potential novel manufacturing method for PTLs to overcome some of the constraints and drawbacks of traditional methods. L-PBF is known to allow exceptional design flexibility while enabling efficient use of material and low energy consumption [7]. AM has already been applied to manufacture electrolyser components such as bi-polar plates [8], LGDLs [9] and fully integrated transport layers [10].

This ongoing study aims to explore the feasibility of L-PBF for the fabrication of porous titanium PTLs and to evaluate their performance in a PEMWE system. This paper presents encouraging preliminary findings of this research. The paper is structured in three main parts. First, we present the methodology for developing, designing, and manufacturing AM-produced porous titanium PTLs. The results section discusses our findings on porosity characteristics, structure-process correlations, and pore morphology. Finally, we evaluate the

performance of the AM-produced PTLs through *in-situ* testing in our lab-scale PEMWE. This performance is then compared to that of a press-sintered PTL, which serves as our benchmark.

2 Methodology

2.1 Design and manufacturing

The first step in developing the AM-produced PTL plates was to determine the L-PBF laser process parameters (consisting of laser power, laser scan speed, layer thickness and laser hatch distance) that achieves porous parts. A feasible L-PBF process parameter window was defined using studies by Bezuidenhout [11] and Kim *et al.* [12]. Design Expert's D-optimal surface response methodology was used to create 20 different process parameters combinations [13].

Spheroidized titanium powder (commercially pure Grade 1) was acquired from AP&C. The manufacturer reports a particle size distribution (by laser diffraction) of 15–45 μm with $D_{10}=17\ \mu\text{m}$, $D_{50}=32\ \mu\text{m}$ and $D_{90}=44\ \mu\text{m}$. The manufacturer further reports an apparent density (ASTM B212) of $2.55\ \text{g}/\text{cm}^3$, flow rate (ASTM B213) of 29 s and an oxygen content $<0.16\%$. A Concept Laser 200R L-PBF machine was used to build plates of 1 mm thickness in a vertical orientation. An initial build, depicted in Figure 1, was done to correlate laser process parameters to part porosity by building 20 mm square samples. After characterising the plates, laser process parameters were selected to build full-sized 71 mm square plates (the required size for installation in the PEM electrolysis system). The criterion for selection was a good build quality and a minimum porosity of 30%.

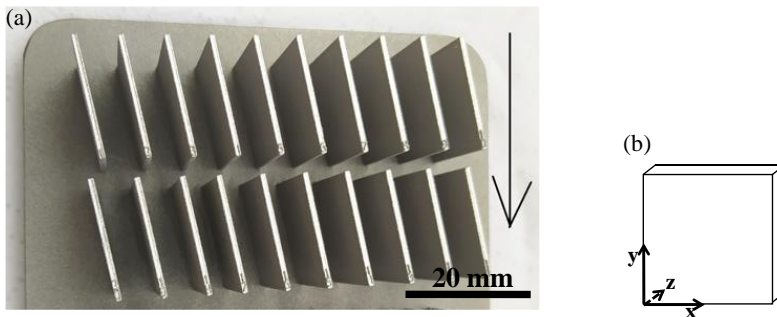


Fig. 1. (a) Photographs of build plate with 20 plate samples (20x20x1 mm). Arrow indicated gas flow and powder coating direction. (b) Sample local coordinate system (*y*-axis is parallel to the build direction and *z*-axis orthogonal to the plate).

2.2 Sample preparation and characterisation

Before characterising and *in-situ* testing, samples were thoroughly cleaned post-fabrication by ultrasonicing twice in acetone for 15 min each (using fresh acetone for each step), followed by 15 min in isopropanol, followed by water for 15 min. Samples were then air-dried. Sample mass was measured post-cleaning using high-precision scale (Kern and Sohn GmbH, model ABT 120-5DM).

To characterise internal porosity and pore morphology, samples were mounted in resin (Struers EpoFix) and placed in a vacuum chamber for 1 hour at 50 kPa below atmospheric pressure to allow for resin impregnation. Samples were then placed in an oven at 40 °C for 24 hours to accelerate curing. Samples were sequentially ground on their *xy*-plane by 320 and 800 grid SiC paper to expose internal pore structures. Mounted samples were then ultrasonically cleaned in iso-propanol for 10 min followed by air-drying.

Micrographs of plates' *xy*-plane was imaged using an Olympus GX51 optical microscope and processed using Stream Essentials software. Sample porosity was estimated by calculated the micrographs' pore-to-solid area ration. This was achieved by stitch multiple neighbouring images to create a large micrograph of ~20 mm². These were converted to black-and-white format. Manual value-thresholding was then applied to determine the ratio of pore area to solid surface area. To calculate an average porosity percentage, this process was repeated on multiple image maps for each sample.

2.3 In-situ performance evaluation

The performance of the L-PBF produced PTLs were evaluated by installing them in their as-fabricated state in a single-cell configuration of a lab-scale PEMWE system. The performance of a commercially available press-sintered PTL plate (71 mm square of 1 mm thickness) was used as a benchmark. The PEMWE system specifications are tabulated in Table 1.

A bi-directional power supply (ITECH electronics – model IT-M3906C-32-240) was used in galvanostatic mode to generate polarization curves. Current step was 0.25 A/s from 0 to 20 A with 5 cycle repetitions. Acquisition resolution is 0.1 s⁻¹. Transient performance was characterised by measuring the current response by applying a voltage step to 2 V (at a rate of 0.01 V/s). A high-resolution acquisition of 0.1 μs⁻¹ was used.

Table 1. PEMWE system specifications.

Component	Specification
Membrane	NAFION N117 (71x71 mm)
Catalyst Coating	IrO ₂ and Pt/C
Bi-polar plate material	Titanium
End-plate material	Stainless steel
Gaskets	Silicone
Water pump inlet pressure [cm]	40-90
Water temperature [°C]	~65
Water flow rate [ml/s]	5
Gas outlet pressure	ambient
Water conductivity [μS]	0.03
Water acidity [pH]	6.2

3 Results

3.1 Internal structure

Figure 2 plots the mass and porosity of the 20 mm square samples as a function of laser energy density (E_v)[†]. As expected, porosity and mass are correlated with E_v the low energy density causes a lack-of-fusion meltpool (see [14]). Mass and porosity data are fitted with a straight line of which the R^2 value of each is printed. The results show that an E_v in the range of 16–17 J/mm³ resulted in a porosity of 18–35%, an E_v of 12–13 J/mm³ resulted in a porosity of 28–40% and an E_v of ~10 J/mm³ resulted in porosity of 44–61%.

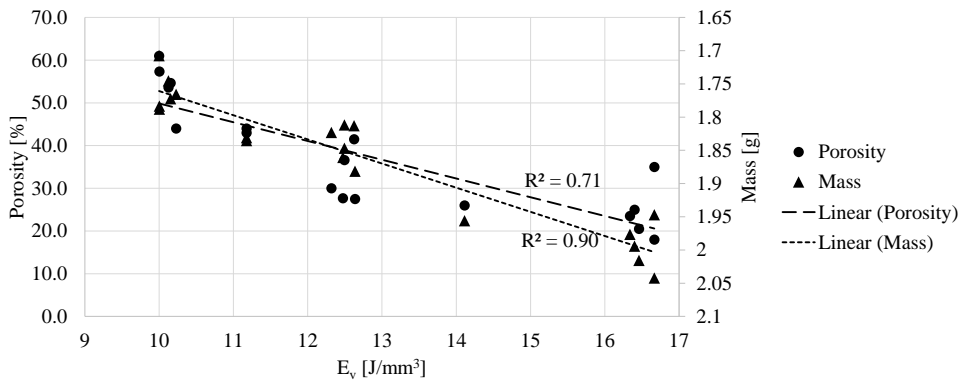


Fig. 2. Sample mass and porosity as a function of E_v .

Process parameters that achieved porosities above 35% (based on the lower threshold recommended by [4]) were selected to produce full-sized plates (i.e., the size required for *in-situ* PEMWE testing). Specification of these samples are tabulated in Table 2 together with the porosity of the benchmark press-sintered PTL plate.

Figure 3 depicts high-magnification optical micrographs of the internal structure of the samples tabulated in Table 2. Although in-depth quantification is required to accurately characterise the internal particle/pore structure, and planned for future work, the following observations can be made when comparing particle / pore sizes and their morphologies. The particles of the press-sintered plates are non-spherical / irregular and more homogeneously distributed, while the free-standing particles of the L-PBF plates are more spherical. The difference in morphology of the particles can be ascribed to the morphology of the starting titanium powder feedstock – the L-PBF process used spheroidized powder, while the sintered plate was made from crushed/milled powder (i.e., irregular powder). The homogenous distribution of the press-sintered particles is due to the homogenous mixing and isometric pressing process.

The sizes press-sintered particles fall in the range of 65–120 μm with some larger free-standing particle measuring ~150 μm (along their longest axis). The AM-produced particles fall in a comparable size range. The x -axis particle measurements are restricted to approximately 75–100 μm (highlighted by the vertical lines on the micrograph). This is caused by the size of the meltpool formed when exposed to the ~75 μm laser spot diameter.

[†] Calculated as $\frac{P}{l \times v \times h}$, where P – laser power, l – layer thickness, v – scan speed and h – hatch distance.

The AM-produced particles are more interconnected in the y -axis (build direction) compared to the x -axis is due to interlayer laser-fusion process. The interconnectedness of the particles is more apparent in the higher E_v sample (S1) since the higher energy density led to a larger number of interlayer fusion compared to the lower E_v samples (e.g., S3). The intermittent lack of inter-layer fusion caused larger pore sizes along the y -axis while pore sizes between scan tracks (x -axis) are comparatively smaller.

Table 2. Full-size PTL specifications.

Sample	E_v [J/mm ³]	Porosity [%]
Press-sintered	n/a	60
AM_S1	12.63	42
AM_S2	10.16	55
AM_S3	10.00	61

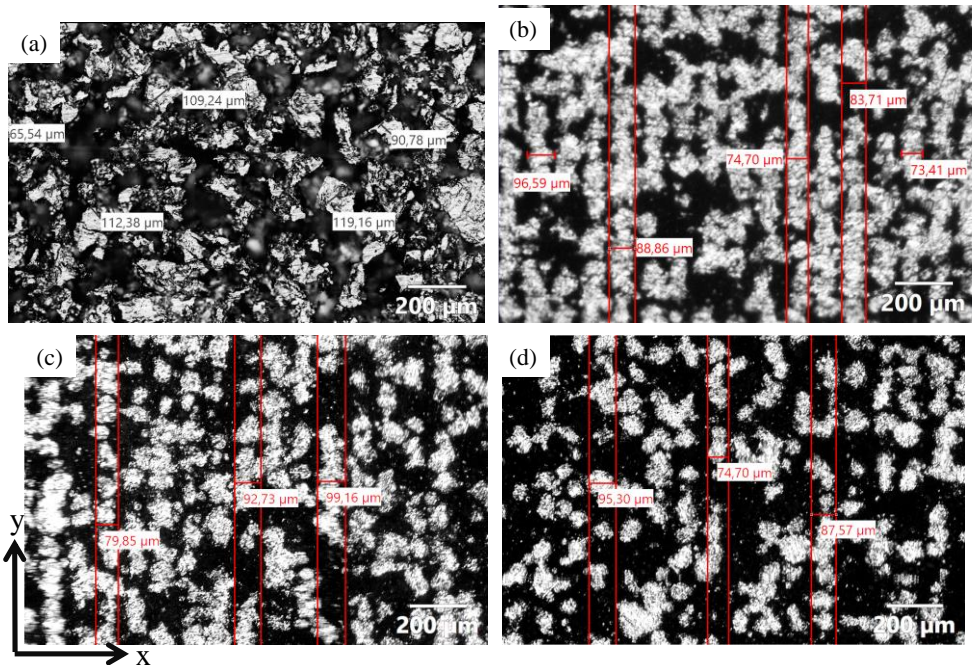


Fig. 3. Optical micrographs of the internal structure of PTLs' xy -planes (a) Press-sintered vs AM-produced samples: (b) S1, (c) S2, (d) S3. Vertical red lines trace interconnected columnar particles. Coordinate system axis (as defined in Figure 1(b)) is included on the bottom left.

3.2 Surface structure

PTL surface structure is a key aspect influencing PEM performance. Figure 4 depicts high-resolution optical micrographs to compare the PTL surface of the (a) press-sintered PTL vs (b, c) AM-produced PTLs. Due to the manufacturing method, the press-sintered PTL has the same external and internal pore structure. Comparatively, the surface of the AM-produced PTLs contain fine sintered powder particles measuring in the range of 20–40 μm (with some larger agglomerated particles). This is in the range of the feedstock powder diameter used for the builds. Therefore, the AM-produced plate has a much finer surface structure – a feature that has been found advantageous in studies of MPLs (see [5]).

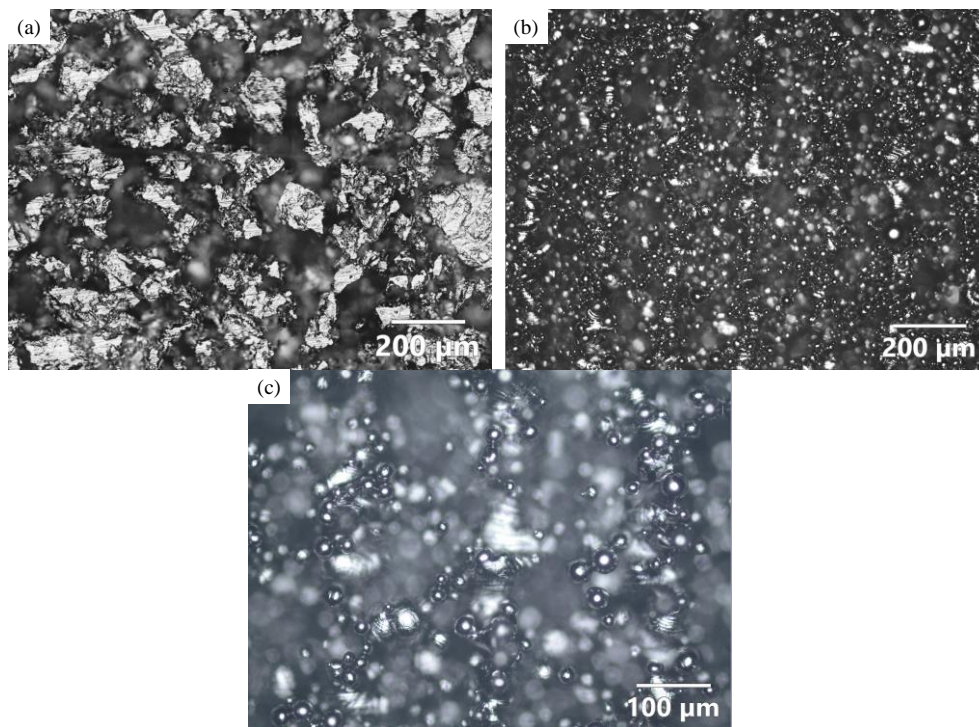


Fig. 4. Optical micrographs of the xy -plane surface of, (a) press-sintered PTL, (b) AM-produced PTL. (c) High-resolution optical micrograph of AM-produced PTL surface.

3.3 *In-situ* PTL performance

Figure 5(a) plots the polarisation curves of the PEMWE cell operating with the PTLs specified in Table 2. Current density was calculated by dividing the measured current data by the surface area of the PTL. Polarization curves show an improvement in performance when using the AM-produced PTL plates compared to the press-sintered plate as indicated by the lower voltage curves achieved by the later. The performance of the three AM-produced plates achieved similar performance with S3 achieving a slightly poorer performance compared to S1 and S3 especially at higher current densities. S1 and S2 achieved near identical results.

Figure 5(b) plots the transient current density of AM-produced plates S1 and S2. The transient current response of the PEMWE provides insight into mass transport efficiency of the electrolyser. A faster rate of current density decrease was produced by S3 compared to S1. This is likely due to a faster rate of accessible water depletion at the CCM-PTL interface attributed to a lower water transport efficient. With an increase in time past 2 seconds (not shown), the difference in current density at steady state voltage becomes apparent which is also reflecting the difference in voltage measured at 0.4 A/cm^2 of the polarisation curves.

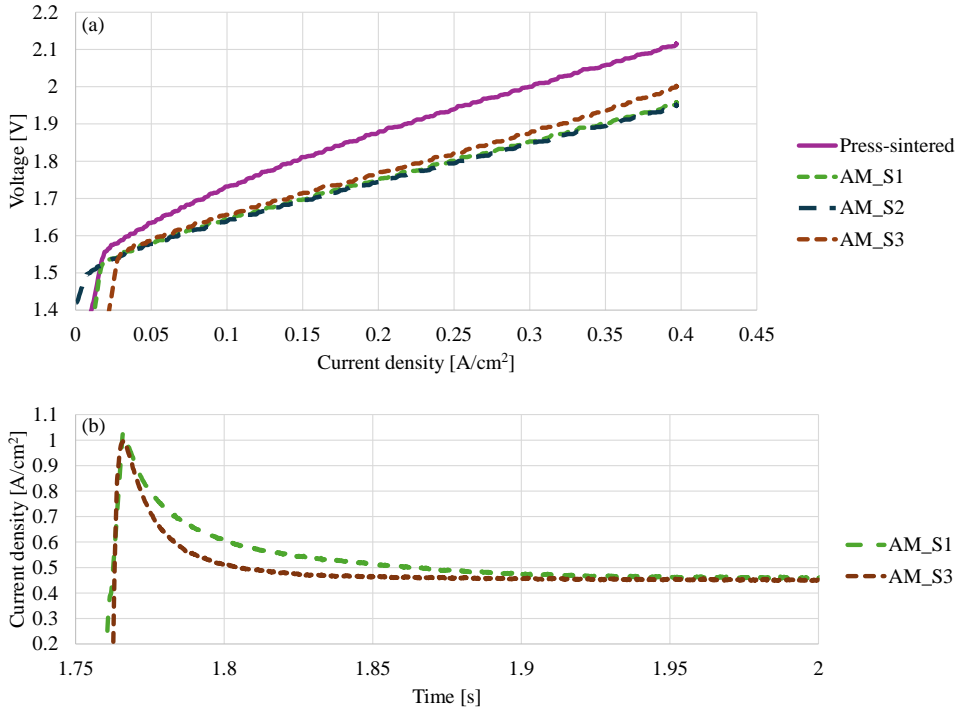


Fig. 5. Performance of the PEMWE comparing press-sintered PTL vs AM-produced PTL, (a) polarization curves, (b) transient current density vs time of AM-produced PTLs.

4 Conclusion

This paper presents encouraging preliminary findings from our ongoing study into the feasibility of L-PBF for fabricating porous titanium PTLs and their performance in PEMWE cells. Our initial results indicate that L-PBF was able to produce 1 mm thick titanium plates with porosity in the recommended range of 30–50%. The internal structure of the AM vs press-sintered plates showed particles of a similar scale in the range of 65–120 μm . Key differences are that AM-produced PTL have more spherical, but textured particle-pore structure compared to an irregular, but homogenous particle-pore structure observed in the press-sintered PTL. Results of the *in-situ* tests of the AM-produced PTLs showed an improved PEMWE performance compared to commercially available press-sintered PTL plates. This improvement is argued to be attributed to the finer surface structure of AM-produced PTLs and their good gas-liquid transport properties. These preliminary findings suggest promising potential for this innovative approach to PTL manufacturing.

This work was supported by the Strategic Fund of Stellenbosch University through the Hydrogen Engineering Research Platform. The authors appreciate and thank Stellenbosch University for its commitment to advancing sustainable hydrogen technologies.

References

- [1] T.L. Doan, H.E. Lee, S.S.H. Shah, M. Kim, C. Kim, H. Cho, T. Kim, A review of the porous transport layer in polymer electrolyte membrane water electrolysis, *Int.*

- J. Energy Res. 45 (2021) 14207–14220. doi:10.1002/er.6739.
- [2] T. Wang, X. Cao, L. Jiao, PEM water electrolysis for hydrogen production: fundamentals, advances, and prospects, Carbon Neutrality. 1 (2022) 1–19. doi:10.1007/s43979-022-00022-8.
- [3] C. Xu, J. Wang, J. Wang, K. Yang, G. Li, W. Gao, H. Wang, S. Zhao, Structural optimization study on porous transport layers of sintered titanium for polymer electrolyte membrane electrolyzers, Appl. Energy. 357 (2024) 122541. doi:10.1016/j.apenergy.2023.122541.
- [4] S.A. Grigoriev, P. Millet, S.A. Volobuev, V.N. Fateev, Optimization of porous current collectors for PEM water electrolyzers, Int. J. Hydrogen Energy. 34 (2009) 4968–4973. doi:10.1016/j.ijhydene.2008.11.056.
- [5] T. Schuler, J.M. Ciccone, B. Krentscher, F. Marone, C. Peter, T.J. Schmidt, F.N. Büchi, Hierarchically Structured Porous Transport Layers for Polymer Electrolyte Water Electrolysis, Adv. Energy Mater. 10 (2020) 1–12. doi:10.1002/aenm.201903216.
- [6] Z. Kang, G. Yang, J. Mo, S. Yu, D.A. Cullen, S.T. Retterer, T.J. Toops, M.P. Brady, G. Bender, B.S. Pivovar, J.B. Green, F.Y. Zhang, Developing titanium micro/nano porous layers on planar thin/tunable LGDLs for high-efficiency hydrogen production, Int. J. Hydrogen Energy. 43 (2018) 14618–14628. doi:10.1016/J.IJHYDENE.2018.05.139.
- [7] A. Baroutaji, A. Arjunan, J. Robinson, M.A. Abdelkareem, A.G. Olabi, Additive manufacturing for Proton Exchange Membrane (PEM) hydrogen technologies: merits, challenges, and prospects, Int. J. Hydrogen Energy. 52 (2024) 561–584. doi:10.1016/J.IJHYDENE.2023.07.033.
- [8] S. Celik, B. Timurkutluk, U. Aydin, M. Yagiz, Development of titanium bipolar plates fabricated by additive manufacturing for PEM fuel cells in electric vehicles, Int. J. Hydrogen Energy. 47 (2022) 37956–37966. doi:10.1016/j.ijhydene.2022.08.282.
- [9] J. Mo, R.R. Dehoff, W.H. Peter, T.J. Toops, J.B. Green, F.-Y. Zhang, Additive manufacturing of liquid/gas diffusion layers for low-cost and high-efficiency hydrogen production, Int. J. Hydrogen Energy. 41 (2016) 3128–3135. doi:10.1016/j.ijhydene.2015.12.111.
- [10] G. Yang, Z. Xie, S. Yu, K. Li, Y. Li, L. Ding, W. Wang, F.-Y. Zhang, All-in-one bipolar electrode: A new concept for compact and efficient water electrolyzers, Nano Energy. 90 (2021) 106551. doi:10.1016/j.nanoen.2021.106551.
- [11] M. Bezuidenhout, Laser Powder Bed Fusion-Centred Approach to Enable Local Drug Delivery from a Cementless Hip Stem, Stellenbosch University, 2021.
- [12] W.R. Kim, G.B. Bang, O. Kwon, K.H. Jung, H.K. Park, G.H. Kim, H.T. Jeong, H.G. Kim, Fabrication of porous pure titanium via selective laser melting under low-energy-density process conditions, Mater. Des. 195 (2020) 109035. doi:10.1016/J.MATDES.2020.109035.
- [13] Design-Expert® software, version 13, (n.d.). <https://www.statease.com/software/design-expert/>.
- [14] G. Ter Haar, Laser powder bed fusion produced Ti-6Al-4V: Microstructural transformations and changes in deformation behaviour through thermal treatments, Stellenbosch University, 2021. <http://hdl.handle.net/10019.1/123601>.